# In vivo tumor angiogenesis imaging with site-specific labeled $^{99m}$Tc-HYNIC-VEGF

Francis G. Blankenberg[1, 2], Marina V. Backer[3], Zoia Levashova[1], Vimalkumar Patel[3], Joseph M. Backer[3]

[1] Division of Nuclear Medicine/Department of Radiology & MIPS (Molecular Imaging Program at Stanford), Stanford University, Stanford, CA 94304, USA
[2] Department of Pediatrics, Stanford University, Stanford, CA 94304, USA
[3] SibTech, Inc., Newington, CT 06111, USA

Published online: 13 May 2006


**Abstract.** *Purpose:* We recently developed a cysteine-containing peptide tag (C-tag) that allows for site-specific modification of C-tag-containing fusion proteins with a bifunctional chelator, HYNIC (hydrazine nicotinamide)-maleimide. We then constructed and expressed C-tagged vascular endothelial growth factor (VEGF) and labeled it with HYNIC. We wished to test $^{99m}$Tc-HYNIC-C-tagged VEGF ($^{99m}$Tc-HYNIC-VEGF) for the imaging of tumor vasculature before and after antiangiogenic (low continuous dosing, metronomic) and tumoricidal (high-dose) cyclophosphamide treatment.
*Methods:* HYNIC-maleimide was reacted with the two thiol groups of C-tagged VEGF without any effect on biologic activity in vitro. $^{99m}$Tc-HYNIC-VEGF was prepared using tin/tricine as an exchange reagent, and injected via the tail vein (200–300 μCi, 1–2 μg protein) followed by microSPECT imaging 1 h later.
*Results:* Sequencing analysis of HYNIC-containing peptides obtained after digestion confirmed the site-specific labeling of the two accessible thiol groups of C-tagged VEGF. Tumor vascularity was easily visualized with $^{99m}$Tc/VEGF in Balb/c mice with 4T1 murine mammary carcinoma 10 days after implantation into the left axillary fat pad in controls (12.3±5.0 tumor/bkg, $n$=27) along with its decrease following treatment with high (150 mg/kg q.o.d. ×4; 1.14±0.48 tumor/bkg, $n$=9) or low (25 mg/kg q.d. × 7; 1.03±0.18 tumor/bkg, $n$=9) dose cyclophosphamide. Binding specificity was confirmed by observing a 75% decrease in tumor uptake of $^{99m}$Tc/biotin-inactivated VEGF, as compared with $^{99m}$Tc-HYNIC-VEGF.
*Conclusion:* $^{99m}$Tc can be loaded onto C-tagged VEGF in a site-specific fashion without reducing its bioactivity. $^{99m}$Tc-HYNIC-VEGF can be rapidly prepared for the imaging of tumor vasculature and its response to different types of chemotherapy.

*Keywords:* VEGF – SPECT – HYNIC – Angiogenesis – Carcinoma

**Eur J Nucl Med Mol Imaging (2006) 33:841–848**
DOI 10.1007/s00259-006-0099-1

Francis G. Blankenberg (✉)
Division of Nuclear Medicine/Department of Radiology & MIPS (Molecular Imaging Program at Stanford),
Stanford University,
Stanford, CA 94304, USA
e-mail: blankenb@stanford.edu
Tel.: +1-650-4978601, Fax: +1-650-4978745

## Introduction

Endothelial cell specific receptors for vascular endothelial growth factor (VEGF), such as VEGFR-2 (KDR/Flk-1), are particularly attractive targets for molecular imaging because they are selectively overexpressed during tumor neovascularization [1–3]. VEGFR-2 is abundantly expressed in tumor vasculature, with approximately 40,000 copies per endothelial cell with a high binding affinity ($K_d$ 50–770 pmol/l) for VEGF [4]. Although VEGF would be a natural choice for the targeted imaging of tumor vasculature, development of VEGF-based radiopharmaceuticals is severely hindered by inactivation of this fragile molecule upon conjugation of bifunctional chelating molecules such as HYNIC [5].

We have previously reported on the development and in vivo imaging characteristics of a VEGF tagged fusion protein for radionuclide imaging of tumor angiogenesis [5]. To load VEGF with $^{99m}$Tc without destructive random modification of the protein with chelating agents, we used a humanized adapter/docking tag system [6]. This system is based on high-affinity interactions between two fragments of human RNase I, a 1–15 aa fragment (Hu-tag) fused to VEGF as a docking tag, and a 21–127 aa fragment (HuS) serving as an adapter protein that was labeled with $^{99m}$Tc. This work demonstrated that stability of $^{99m}$Tc-HuS/Hu-VEGF complexes is sufficient for mouse imaging and established the feasibility of imaging VEGF receptors as

molecular markers of angiogenesis with contrast agents directed by functionally active VEGF. However, this adapter/docking tag system may be much less effective for clinical imaging owing to the increased dissociation of injected complexes in the larger blood pool of humans as compared with mice. To develop $^{99m}$Tc-labeled VEGF that is not corrupted by random modification and is suitable for human use, we expressed VEGF with a novel cysteine-containing peptide tag, named C-tag, which was engineered by R4C substitution in Hu-tag [7]. As in a previous study [5], we based our construct on $VEGF_{121}$, a circulating form of VEGF that does not contain heparin-binding domain. The heparin-binding domain found in other forms of VEGF causes the protein to be non-specifically sequestered in the extracellular matrix, thereby reducing the soft tissue clearance and decreasing the target to background tracer uptake ratio.

We now report on how the C4 thiol group in C-tagged VEGF can be derivatized with HYNIC (hydrazine nicotinamide) without a significant effect on VEGF's functional activities. Furthermore, we show that HYNIC-VEGF can be rapidly loaded with $^{99m}$Tc, creating a new VEGF-directed radiotracer, $^{99m}$Tc-HYNIC-VEGF. We found that this agent can reveal the heterogeneity of tumor vasculature in an orthotopic mouse model of mammary adenocarcinoma, and its response to low-dose metronomic (antiangiogenic) and high-dose (tumoricidal) cyclophosphamide treatment.

## Materials and methods

### *4T1 murine tumor model*

Female Balb/c mice were obtained from the breeding facility of the Department of Comparative Medicine, Stanford University. All mice were between 6 and 8 weeks in age. Care of all experimental animals was in accordance with institutional guidelines and approved protocols, and animals were housed and treated in a humane manner in strict accordance with Department of Agriculture and institutional animal subject guidelines (NIH publication No. 86-23, revised 1985). $5\times10^5$ 4T1 murine mammary adenocarcinoma cells were directly implanted into the left axillary mammary fat pad. On day 10 after implantation, treated animals were divided into two groups: high dose =150 mg/kg i.p. q.o.d. (four total doses) ($n$=9) or low dose =25 mg/kg i.p. q.d. (seven total doses) ($n$=9). On day 17 all treated mice were imaged and sacrificed for biodistribution and histology assay. Fourteen mice were left untreated after day 8 and followed by imaging and sacrifice on day 14, with removal of tumor for scintillation well counting and histologic assay. An additional 20 tumor-bearing mice at day 10 were used for biodistribution assay of tracer and radiolabeled control protein. Five normal Balb/c mice were used for determination of blood clearance of tracer. Mice were all sacrificed via $CO_2$ inhalation according to IRB animal guidelines.

### *Generation of recombinant tagged C4-VEGF fusion protein*

The pET/Hu($G_4$S) vector for expression of recombinant proteins with an N-terminal Hu-tag fused to protein ORF via a $G_4$S linker was constructed as described elsewhere [8]. C-tag was created by introduction of the R4C amino acid substitution in Hu-tag by site-directed mutagenesis (Gene-Tailor Site Directed mutagenesis kit, Invitrogen) using primers: 5′- AT ATA CAT ATG AAA GAA TCT *TGC* GCT AAA AAA TTT C (sense, mutation italicized) and 5′–AGA TTC TTT CAT ATG TAT ATC TCC TTC TTA AAG TT (antisense). The resultant pET/Hu-R4C($G_4$S) vector was confirmed by sequencing. A 3–112 fragment of the 121-aa isoform of human VEGF was cloned into pET/Hu-R4C($G_4$S). C-tagged VEGF (C-VEGF) was expressed and purified as described for Hu-tagged recombinant VEGF elsewhere [9]. To obtain free SH groups, C-VEGF was incubated with a 1.5-fold molar excess of DTT in 0.1 *M* Tris-HCl pH 8.0, 0.5 *M* urea, 0.5 *M* NDSB-221 for 16 h at 4°C, and desalted. Free SH groups were detected by a reaction with *N*-(1-pyrene)-maleimide (Molecular Probes, Eugene, OR, USA), as described elsewhere [5, 7, 9].

### *Linking C4-VEGF protein to HYNIC and in vitro testing*

C-tagged VEGF was mixed with dimethylformamide dissolved 5-maleimido-2-hydraziniumpyridine hydrochloride (HYNIC-maleimide) at the molar HYNIC/protein ratio of 3:1 in a buffer containing 20 m*M* Tris HCl pH 8.0 and incubated for 1 h at room temperature. The product, designated HYNIC-VEGF, was purified on PD-10 column (Amersham, USA) equilibrated with 0.114 *M* tricine, pH 6.9. The concentration of protein and HYNIC was determined by reversed phase high-pressure liquid chromatography (RP HPLC) by measuring the integral optical density of the HYNIC-VEGF peak at 216 nm and 310 nm, respectively. Under the selected conditions, the ratio of HYNIC to VEGF in purified HYNIC-VEGF was ~1. The site of HYNIC conjugation was confirmed by N-terminal sequencing of purified HYNIC-containing peptides obtained after digestion of HYNIC-VEGF with AspN protease (Sigma). A negative protein control for tumor uptake of HYNIC-VEGF was generated by the inactivation of C-tagged VEGF activity (>99%, data not shown) through the excessive biotinylation of the protein with a 90-fold molar excess of sulfo-NHS-LC-Biotin (Pierce) for 1 h in 20 mM NaOAc pH 6.5, followed by desalting. Biotin-inactivated C-tagged VEGF was then modified with HYNIC as described above.

### *In vitro assays of HYNIC-VEGF activity*

HEK293 human transformed embryonic kidney cells (CRL-1573) were from the American Type Culture Collection (Manassus, VA, USA). 293/KDR cells expressing $2.5\times10^6$ VEGFR-2/cell are described elsewhere [10]. VEGFR-2 tyrosine autophosphorylation in 293/KDR cells was performed as described elsewhere [7]. Briefly, cells were plated into 24-well plates, $7.5\times10^4$ cells/well, shifted to starvation medium (DMEM/0.5% FBS) 6 h later, and incubated for 16 h at 37°C in 5% $CO_2$. Then cells were switched to serum-free DMEM with 0.5 m*M* sodium vanadate for 20 min at 37°C, stimulated with VEGF for 10 min at 37°C, lysed, and analyzed by Western blotting using anti-phosphotyrosine RC20 antibody conjugated to horseradish peroxidase (BD Transduction Labs, San Diego, CA, USA).

SLT-VEGF fusion toxin ($VEGF_{121}$ fused to the Shiga-like toxin subunit A) was prepared as described previously [11]. SLT-VEGF protection assay was performed as described elsewhere [5, 7]. Briefly, 293/KDR cells were plated on 96-well plates, 1,000 cells/well. C-VEGF or HYNIC-VEGF was mixed with SLT-VEGF in complete culture medium and added to cells in triplicate wells to a final SLT-VEGF concentration of 1 n*M*. Cells were quantitated 96 h later by CellTiter 96 $AQ_{ueous}$ One Solution Cell Proliferation Assay kit (Promega, USA).

*Radiolabeling of imaging complexes*

HYNIC-VEGF and HYNIC-biotin-inactivated VEGF were radiolabeled using [$^{99m}$Tc]-tricine as a precursor complex [12]. After 1 h of incubation at room temperature radiolabeled protein was run on a PD10 Sephadex-25 gel filtration column eluted with PBS (1× phosphate-buffered saline). Specific activities routinely ranged from 3.7 to 7.4 MBq/μg protein with a radiopurity of greater than 95%.

*Clearance and biodistribution studies*

All Balb/c mice received injections of 18.5–37 MBq (2–5 μg of protein) of $^{99m}$Tc-HYNIC- VEGF via the tail vein. For blood clearance studies, five normal animals were sedated with ketamine (100 mg/kg i.p.) (Fort Dodge, IA, USA) and xylazine (10 mg/kg, i.p.) (Butler, Columbus, OH, USA). Blood aliquots (<50 μl) were then obtained at 1, 5, 10, 30, and 60 min after tail vein injection of tracer via serial supra-orbital venous sampling of mice while under sedation.

Biodistribution assay was then performed with four separate groups of un-anesthetized tumor-bearing mice ($n$=5 mice per group) injected with either $^{99m}$Tc-HYNIC-VEGF or $^{99m}$Tc-HYNIC-biotin-inactivated VEGF [18.5–37 MBq (2–5 μg of protein)]. Mice injected with $^{99m}$Tc-HYNIC-biotin-inactivated VEGF served as a negative protein control group for non-specific tumor uptake. These four groups of mice were then sacrificed for determination of tracer distribution at 1 or 4 h after injection.

Tissue and organ samples were analyzed with a scintillation well counter along with three samples of standard activity (1/100 of injected dose) at an energy level of 140 keV and an energy window of ±20 keV. Results are expressed as the average of the percentage of injected dose (ID) per gram (g) of tissue ± one standard deviation of the mean. A two-tailed Student's $t$ test with an equal variance was used to calculate significance at a $p$ value of less than 0.05.

*Small animal SPECT imaging*

For imaging, mice were anesthetized as for the blood clearance study above. One hour prior to radionuclide imaging, 18.5–37 MBq of $^{99m}$Tc-HYNIC-VEGF was injected via the tail vein. Radionuclide imaging was performed with a small animal SPECT imaging gamma camera (LumaGEM single head A-SPECT; Gamma Medica, LA) using a 1-mm pinhole collimator (360° of rotation, 15 s per 3° step, and a 64×64 imaging matrix with an imaging time of approximately 13 min per animal). Data were reconstructed using commercially available software (Mirage Software, version 5.3, Segami Corporation, Columbia, MD, USA) into a $64^3$ three-dimensional imaging matrix from which 1.2-mm-thick axial slices through the left axillary tumor were extracted with a voxel size of 1.2×1.2×1.2 mm [13–15]. Immediately after radionuclide imaging, tumor-bearing mice were sacrificed for limited biodistribution analysis (i.e. tumor, blood, soft tissue, muscle). Region of interest (ROI) image analyses were performed on both planar and reconstructed axial SPECT image using Mirage Software, version 5.3. Activities from the axial SPECT ROI image analyses were expressed as counts/pixel.

*Immunohistochemistry of 4t1 mammary tumors*

Tumors were mounted in TissueTEK OCT compound (Miles Inc., Elkhart, IN, USA), snap-frozen in liquid nitrogen and stored at −70°C until required. Cryosections of 7 μm were cut serially through the entire tumor. The sections were fixed with 1% formaldehyde (Polysciences, Warrington, PA, USA) for 10 min at room temperature, and stained for endothelial specific markers after quenching of endogenous peroxidase with 0.3% $H_2O_2$ for 10 min at room temperature. For chromogenic detection, slides were blocked in 5% normal rabbit serum, incubated with CD31 (PECAM) or VEGFR-2 (KDR/Flk-1) rat anti-mouse antibodies (Pharmingen, San Diego, CA, USA), followed by incubation with rabbit-anti rat biotinylated secondary antibody pre-absorbed on mouse tissue (Vector Labs, Burlingame, CA, USA). Secondary antibodies were coupled with peroxidase using the Elite streptavidin-biotin complex kit (Vector Labs), visualized with DAB (Vector Labs) according to the manufacturer's instructions, counterstained with methyl green (Vector Labs) diluted tenfold with water, and mounted with Histomount (Vector Labs). Microscopic images were obtained with a Zeiss Axiovert inverted microscope at original magnification x40. Images were processed using Adobe Photoshop software (Adobe Systems Incorporated, San Jose, CA, USA). For quantitative analysis, microscopic images obtained from five randomly selected fields were converted to grayscale. The tonal range of the grayscale images of sections stained in the same experiment was adjusted to the same high and low levels in order increase contrast. The selected images were binarized to black and white with the same threshold that preserves immunostaining visible by eye as black pixels on a white background. Immunostained areas in binarized images were quantitated by histogram analysis.

## Results

*Preparation of C-tagged VEGF and HYNIC-VEGF*

C-tagged VEGF was constructed by fusion 1–15 aa fragment of human RNase I with R4C substitution to 3–112 fragment of human $VEGF_{121}$ via a $G_4S$ linker. Construction, expression, and purification followed procedures described recently for the full-length recombinant $VEGF_{121}$ [7]. A shorter fragment of $VEGF_{121}$ was chosen to avoid potential problems associated with presence of cysteine in position 116 in the full-length $VEGF_{121}$. After refolding in standard glutathione/oxidized glutathione redox buffers, we obtained a functionally active protein, with 90–100% C4 thiol groups forming mixed disulfides with glutathione (see Materials and methods for details). We found that the thiol groups in C-tagged VEGF can be "deprotected" under relatively mild reducing conditions (see Materials and methods) and thus made available for site-specific conjugation with HYNIC-maleimide. HYNIC-VEGF was then purified by gel filtration and the site of conjugation was confirmed by digestion of purified conjugate with AspN protease, RP HPLC purification of HYNIC-containing peptides, and N-terminal amino acid sequencing of these peptides.

*Testing HYNIC-VEGF in tissue culture*

VEGF binds to and induces tyrosine autophosphorylation of its receptor VEGFR-2. We found that HYNIC-VEGF induced VEGFR-2 tyrosine autophosphorylation in VEGFR-2 expressing 293/KDR cells with an efficiency similar to that of parental VEGF (Fig. 1a). HYNIC-VEGF was also active in protection of 293/KDR cells from VEGFR-2 mediated cytotoxicity of SLT-VEGF fusion toxin (Fig. 1b) that combines $VEGF_{121}$ and the catalytic subunit of Shiga-like toxin [11]. Both assays indicated that VEGF moiety in HYNIC-VEGF conjugate retained its full ability to bind to VEGFR-2.

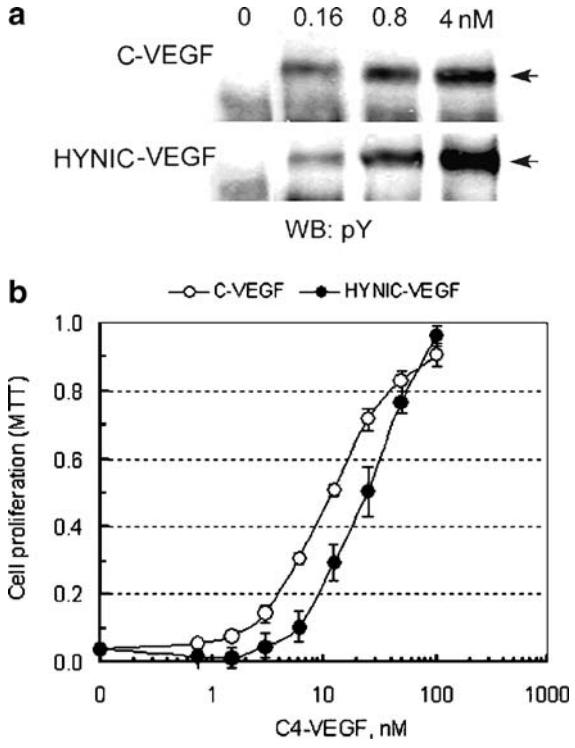


**Fig. 1. a, b** Functional activity of HYNIC-VEGF conjugate. For both assays, 293/KDR cells expressing $2\times10^6$ VEGFR-2/cell were used. (**a**) VEGFR-2 tyrosine autophosphorylation assay. Near confluent cells after 16-h starvation (DMEM/0.5% FBS) were stimulated with the indicated concentrations of HYNIC-VEGF or VEGF and analyzed by Western blotting. *Arrows* indicate positions of VEGFR-2. This assay showed that increases in the concentration of C4-VEGF and C4-VEGF labeled with HYNIC stimulated enzymatic activity to the same degree. (**b**) Rescue of cells from SLT-VEGF induced cytotoxicity. In this figure unlabeled C4-VEGF (*open circles*) and HYNIC-labeled C4-VEGF (*solid circles*) were titrated against SLT-VEGF (i.e., *Shigella* toxin-labeled VEGF that is lethal once bound and internalized in 293/KDR cells) in a competition assay. Note that with similar increases in C4-VEGF and HYNIC-C4-VEGF concentration, a nearly identical effect is seen on the survival (cell proliferation viability as measured by the MTT assay), confirming that modification of C4-VEGF with HYNIC did not affect its biologic activity in vitro

*Blood clearance in normal mice*

$^{99m}$Tc-HYNIC-VEGF was rapidly cleared from the blood in a bi-exponential fashion with a rapid component in the first 10 min followed by a significantly slower component thereafter, as shown in Fig. 2.

*Biodistribution studies in tumor-bearing mice*

Results of biodistribution assays performed on tumor-bearing mice are shown in Fig. 3. Tumor uptake of $^{99m}$Tc-HYNIC-VEGF was two- and fourfold greater than the uptake of $^{99m}$Tc-HYNIC-biotin-inactivated VEGF at 1 and 4 h, respectively. There was no significant change in tumor (or other organ or tissue) uptake of $^{99m}$Tc-HYNIC-VEGF between 1 and 4 h after injection, with the exception of blood pool activity, which decreased from 1.03±0.32% to 0.68±0.38% ID/g, respectively. Of note, sedation appeared to prolong the clearance of $^{99m}$Tc-HYNIC-VEGF with an average blood pool activity of 3.36±1.12% ID/g at 1 h in sedated normal mice undergoing serial venous sampling which was threefold greater than observed in non-sedated tumor-bearing mice.

In mice injected with $^{99m}$Tc-HYNIC-biotin-inactivated VEGF, however, there was a significant loss of tracer from tumor between 1 and 4 h after injection (1.95±1.33% to 0.92±0.59% ID/g, respectively), presumably due to wash-out of unbound control protein which paralleled the decrease in blood pool activity (1.46±0.11% to 0.52± 0.07% ID/g, respectively).

With respect to other organs and tissues, the kidneys had the highest uptake of $^{99m}$Tc-HYNIC-VEGF followed by intermediate levels of tracer observed within the lungs, liver, and spleen. The majority of renal uptake was found within the renal cortex, with little excretion into the renal collecting system, in a fashion similar to other HYNIC-labeled proteins (data not shown). Stomach, bowel, skeletal muscle, thymus and heart had the lowest levels of tracer uptake.

*Small animal SPECT imaging of tumor-bearing mice*

There was markedly increased circumferential (rim) uptake of tracer in the pre-treatment scans of tumor-bearing mice that exceeded the actual dimensions of mammary fat pad tumor (average tumor diameter 9.0±2.1 mm, $n$=32) as shown in Fig. 4. Most likely, this enhancement reflects overexpression of VEGF receptors at the edges of growing tumors that provides for receptor-mediated uptake and internalization of VEGF-driven contrast agents.

To establish whether imaging with $^{99m}$Tc-HYNIC-VEGF can detect effects of chemotherapy on tumor vasculature, mice were treated with high (tumoricidal) and daily low (metronomic) dose cyclophosphamide therapy. We observed that tumor size remained relatively unchanged after 7 days of low- or high-dose therapy, as compared with pre-treatment values (9.6±1.9 and 9.9±2.1 mm vs 9.0±2.1 mm, respec-

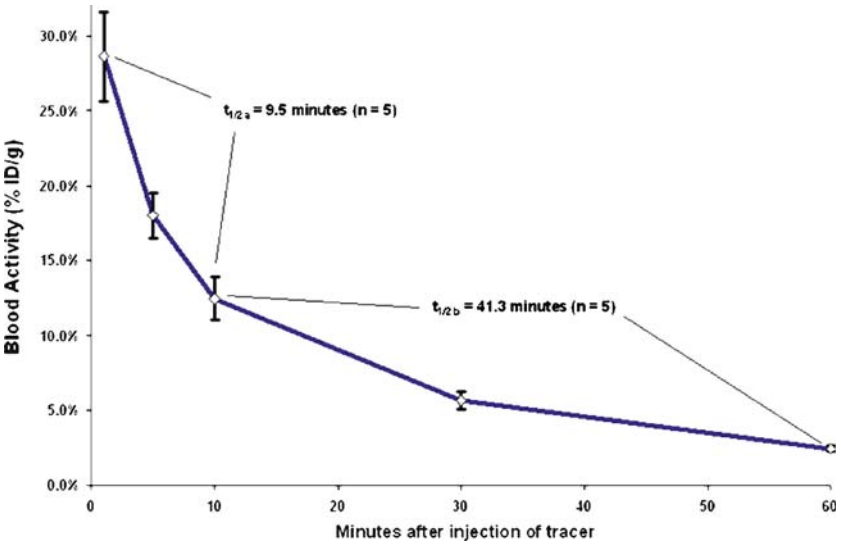


**Fig. 2.** Blood clearance of tracer. The specific activity of serial blood samples drawn through supra-orbital venous plexus after tail vein injection of 18.5 MBq (2–5 μg of protein) of $^{99m}$Tc-HYNIC-VEGF. Results are expressed as % injected activity per gram of blood versus time after injection expressed in minutes. *Error bars* represent one standard deviation from the mean of five mice. The blood clearance of tracer was best described by a bi-exponential function with a fast first component ($t_{1/2}$=9.5 min) in the first 10 min after injection of tracer and a much slower component ($t_{1/2}$=41.3 min) in the remaining 50 min

tively). Both treatment regimens resulted in similar decreases in tracer uptake, as shown in Fig. 5. The pattern of decreased tracer uptake consisted of a general decrease in the amount of radioactivity retained within tumor accompanied by the near-complete disappearance of focal rim activity (well-defined peripheral uptake). These results were confirmed at ROI analyses in which there was a disappearance of rim activity and a two- to threefold decrease in total tumor uptake after 7 days of either low- or high-dose cyclophosphamide therapy.

Biodistribution assay also showed a significant decrease ($p$<0.001) in average tumor uptake of tracer in the low-dose and high-dose treatment groups with activities of 1.09± 0.72% and 1.22±0.70% ID/g, respectively, as compared with control (untreated) tumor (2.94±0.45% ID/g). The relatively lower tumor uptake in animals undergoing SPECT imaging as compared with that seen in the groups undergoing biodistribution assay (4.20±0.78% ID/g at 1 h and 4.07±0.34% ID/g at 4 h) most likely was due to the larger tumor size in the imaging group (0.45±0.23 vs 0.08± 0.03 g, respectively). This appeared to be confirmed by a weak but significant ($p$<0.01) negative linear correlation of

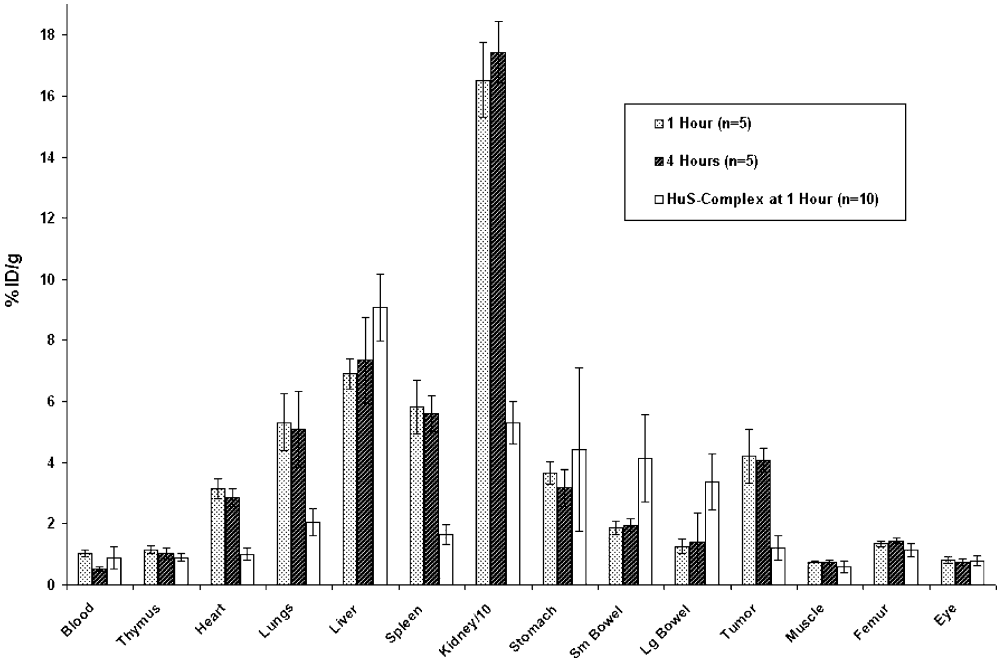


**Fig. 3.** Biodistribution in tumor-bearing mice. Separate groups of five tumor-bearing mice were sacrificed 1 or 4 h after tail vein injection of 18.5 MBq (2–5 μg of protein) of $^{99m}$Tc-HYNIC-VEGF. Activity of each specimen was determined as for blood clearance studies and expressed as % injected dose per gram of tissue. *Stippled bars* represent the average of the group of mice sacrificed at 1 h, the *gray bars* represent the 4-h group, and the *clear bars* are the biodistribution data at 1 h from a previously published article [5] using $^{99m}$Tc-HuS/Hu-VEGF (HuS-Complex) in tumor-bearing adult Balb/c mice ($n$=10). *Error bars* represent one standard deviation from the mean value of uptake for each tissue

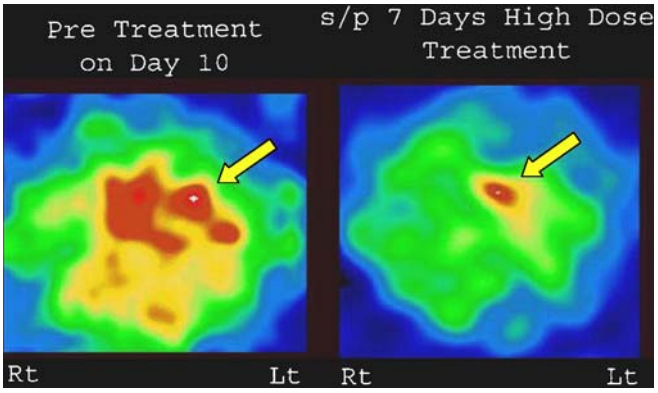


**Fig. 4.** SPECT imaging pre and post high-dose cyclophosphamide. Representative axial (transverse) radionuclide images from a 4T1 tumor-bearing mouse 10 days following implantation of $5\times10^5$ cells into the mammary fat pad next to the left axilla. Images were obtained 1 h after injection of 37 MBq (4 μg of protein) of $^{99m}$Tc-HYNIC-VEGF injected via the tail vein. *Arrows* mark the location of tumor uptake before and after treatment. *Rt* right, *Lt* left. Images are displayed with tracer activity coded on a pseudo-color scale with white and red having the highest intensity of focal activity while green and blue were the lowest. Note the almost complete disappearance of high rim activity of implanted tumor (red semicircle of intense focal uptake surrounding a relatively lower yellow core) after 7 days of high-dose therapy

tumor weight ($r$=−0.45) with tumor uptake (expressed as% ID/g) as seen at biodistribution assay at the time of sacrifice 1 h after injection of tracer.

### *Immunohistochemical staining and correlation with $^{99m}$Tc-HYNIC-VEGF tumor uptake*

Typically, information on tumor angiogenesis is obtained by immunohistochemical analysis of representative tumors. To compare information obtained by in vivo SPECT imaging with that obtained by immunohistochemical analysis, representative large and small tumors were cryosectioned and immunostained for pan-endothelial marker CD31 and for VEGFR-2, whose levels of expression are high enough for chromogenic visualization only in a subset (~10%) of CD31-positive cells (Backer et al., manuscript in preparation). We found that CD31 abundance in selected tumors was not affected by treatment with cyclophosphamide (Fig. 6a). In contrast, VEGFR-2 abundance was decreased in small tumors after treatment with high-dose cyclophosphamide, and in large tumors after treatment with either low or high cyclophosphamide doses (Fig. 6b). Taken together these results indicate that cyclophosphamide treatment was depleting a subset of tumor endothelial cells that overexpress VEGFR-2, while the majority of CD31-positive cells were unaffected. On the other hand, since cells with the highest VEGFR-2 levels are most likely responsible for $^{99m}$Tc-HYNIC-VEGF binding/uptake, these findings qualitatively agree with SPECT imaging observations that cyclophosphamide treatment decreases $^{99m}$Tc-HYNIC-VEGF tumor uptake.

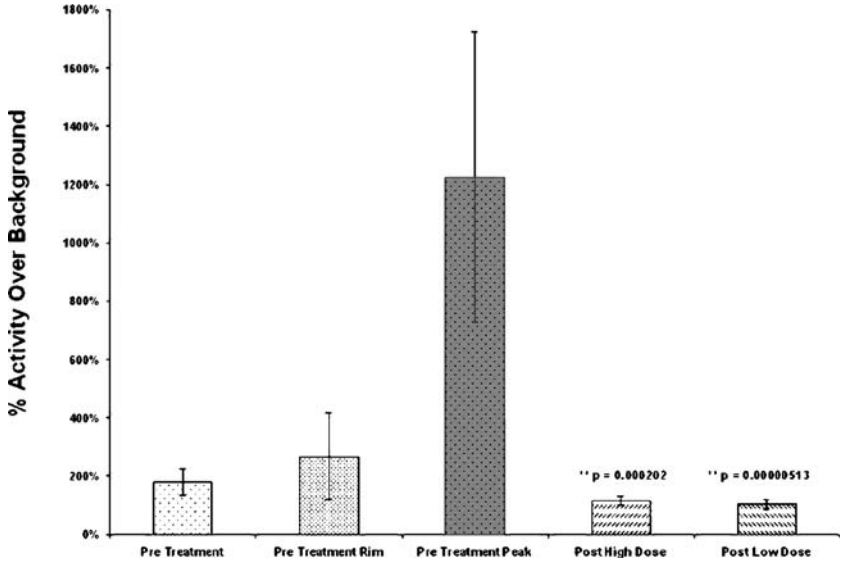


**Fig. 5.** ROI analyses of high- and low-dose cyclophosphamide therapy. Regional activity of the rim and whole tumor was obtained from axial SPECT images of a total of 32 tumor-bearing mice. Two subgroups of nine tumor-bearing mice then underwent 1 week of high- or low-dose cyclophosphamide therapy and were then re-imaged prior to sacrifice. Tumor uptake was expressed as the percent activity (counts/pixel) divided by soft tissue background uptake (counts/pixel) multiplied by 100 (% activity above background). *Error bars* represent one standard deviation from mean values. **Highly significant $p$ value. *Pre Treatment*, whole tumor uptake before treatment; *Pre Treatment Rim*, circumferential focally increased rim of tracer uptake before treatment; *Pre Treatment Peak*, maximal value of activity within the rim of tracer uptake in the periphery of tumor prior to treatment; *Post High Dose*, whole tumor uptake after high-dose therapy; *Post Low Dose* whole tumor uptake after low-dose therapy. Note the rim of tracer uptake could not be defined on SPECT imaging after high- or low-dose therapy, thereby limiting ROI analyses to that of the whole tumor

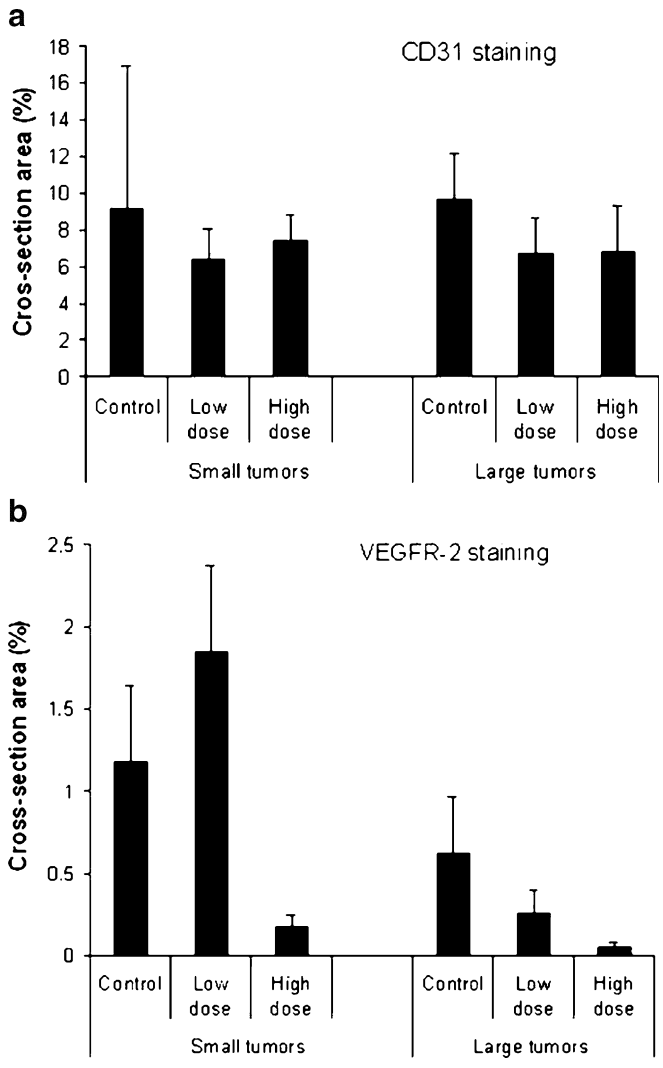


**Fig. 6. a, b** Immunohistochemical analysis of high- and low-dose chemotherapy. Selected tumors from pre-treatment and treated groups were cryosectioned (7 μm) and immunostained for the pan-endothelial cell marker CD31 (**a**) and for VEGFR-2 (**b**), as described in Materials and methods. The immunostaining patterns from five random microscopic fields on individual cryosections were quantified and averaged as described in Materials and methods. *Error bars* represent one standard deviation from the mean value (*solid bars*)

## Discussion

In this manuscript we describe the synthesis, in vitro testing, and initial in vivo validation of $^{99m}$Tc-HYNIC-VEGF as a molecular imaging marker of VEGF receptor density, a crucial feature of tumor angiogenesis. Development of a short cysteine-containing fusion tag allowed for the site-specific conjugation of the bifunctional chelator molecule, HYNIC, to C-tagged VEGF in a way that does not affect the functional domains of VEGF. The expression of VEGF with the C-tag followed by a site-specific conjugation of contrast agents via a standardized non-destructive procedure could serve as a useful paradigm for the synthesis and labeling of other fragile proteins for targeted imaging.

Blood clearance and biodistribution assays with $^{99m}$Tc-HYNIC-VEGF were similar to our previous results with $^{99m}$Tc-HuS/Hu-VEGF complex assembled via a non-covalent adapter/docking tag system [5]. Again, the highest uptake was found within the renal cortical tubular cells, mostly likely due to the cleavage and non-specific intracellular retention of the $^{99m}$Tc-HYNIC adduct.

Imaging of orthotopic mouse mammary 4T1 carcinomas revealed that $^{99m}$Tc-HYNIC-VEGF is preferentially accumulated at the tumor rim, where the most extensive angiogenesis takes place. Indeed, we have reported a similarly enhanced circumferential uptake with near-infrared fluorescent imaging of subcutaneous 4T1 tumors using VEGF/Cy5.5 conjugates [7]. In this previous investigation, C-tagged VEGF labeled at the C4 thiol group with near-infrared fluorescent Cy5.5 dye accumulated at the rim of 4T1 tumors. The specificity of uptake was confirmed by confocal microscopy of tumor cryosections revealing colocalization of C-tagged VEGF-Cy5.5 fluorescence and intense VEGFR-2 immunofluorescent staining in this area [16].

The specificity of C-tagged VEGF binding to tumor vasculature in this current investigation is supported by the observation of a greater than fourfold tumor uptake above the inactive protein control levels 4 h after injection of tracer.

SPECT imaging with $^{99m}$Tc-HYNIC-VEGF can also readily detect the effects of cyclophosphamide treatment on 4T1 tumors. A surprising result from our in vivo modeling of low- (metronomic) and high-dose cyclophosphamide (tumoricidal) was the virtually identical anti-tumor effects and reduction of VEGF tumor uptake after 1 week of therapy. Our results suggest that both treatments result in depletion of cells capable of binding and sequestering $^{99m}$Tc-HYNIC-VEGF. Qualitatively, immunohistochemical analysis of selected tumors supports the notion of cyclophosphamide-induced selective depletion of VEGFR-2-overexpressing cells from tumor neovasculature. These results are particularly significant because there is renewed interest in using certain standard chemotherapeutic agents given at low doses for selective inhibition of the growth of tumor vascular endothelial cells that, for reasons that are unclear, are more sensitive to certain therapies than normal host tissue and tumor cells [17]. The benefits of low-dose metronomic chemotherapy are the selective targeting of tumor vasculature (as a single agent or in combination with other drugs) with absent or moderate toxic effects on the most sensitive target cell populations normally affected by maximally tolerated high-dose therapy (i.e., bone marrow progenitors, gut mucosa, and hair follicle cells). Furthermore, early clinical studies have found no negative impact on wound healing or evidence of organ toxicity with patients undergoing low-dose metronomic cyclophosphamide therapy for metastatic breast cancer [18].

Our imaging results with $^{99m}$Tc-HYNIC-VEGF support the use of low-dose metronomic cyclophosphamide therapy for the selective targeting of tumor endothelial cells.

More generally, our results indicate that imaging VEGF receptors with $^{99m}$Tc-HYNIC-VEGF yields a novel, potentially useful, surrogate marker for this and other types of anti-angiogenic therapy.

*Acknowledgements.* The work was supported by 1R43 CA113080 and 1 R21 EB001946 to J. Backer.

## References


1. Ferrara N. Vascular endothelial growth factor: basic science and clinical progress. Endocr Rev 2004;25:581–611
2. Underiner TL, Ruggeri B, Gingrich DE. Development of vascular endothelial growth factor receptor (VEGFR) kinase inhibitors as anti-angiogenic agents in cancer therapy. Curr Med Chem 2004;11:731–745
3. Hristov M, Erl W, Weber PC. Endothelial progenitor cells: mobilization, differentiation, and homing. Arterioscler Thromb Vasc Biol 2003;23:1185–1189
4. Dvorak HF. Vascular permeability factor/vascular endothelial growth factor: a critical cytokine in tumor angiogenesis and a potential target for diagnosis and therapy. J Clin Oncol 2002;20:4368–4380
5. Blankenberg FG, Mandl S, Cao YA, O'Connell-Rodwell C, Contag C, Mari C, et al. Tumor imaging using a standardized radiolabeled adapter protein docked to vascular endothelial growth factor. J Nucl Med 2004;45:1373–1380
6. Backer MV, Gaynutdinov TI, Gorshkova II, Crouch RJ, Hu T, Aloise R, et al. Humanized docking system for assembly of targeting drug delivery complexes. J Control Release 2003;89:499–511
7. Backer MV, Gaynutdinov TI, Patel V, Bandyopadhyaya AK, Thirumamagal BTS, Tjarks W, et al. Vascular endothelial growth factor selectively targets boronated dendrimers to tumor vasculature. Mol Cancer Ther 2005;4:1423–1429
8. Backer MV, Elliot J, Gaynutdinov TI, Backer JM. Assembly of targeting complexes driven by a single-chain antibody. J Immunol Meth 2004;289:35–43
9. Backer MV, Aloise R, Przekop K, Stoletov K, Backer JM. Molecular vehicles for targeted drug delivery. Bioconjug Chem 2002;13:462–467
10. Backer MV, Backer JM. Functionally active VEGF fusion proteins. Prot Express Purif 2001;23:1–7
11. Backer MV, Backer JM. Targeting endothelial cells over-expressing VEGFR-2: selective toxicity of Shiga-like toxin-VEGF fusion proteins. Bioconj Chem 2001;12:1066–1073
12. Larsen SK, Solomon HF, Caldwell G, Abrams MJ. [$^{99m}$Tc] tricine: a useful precursor complex for the radiolabeling of hydrazinonicotinate protein conjugates Bioconjugate Chemistry 1995;6:635–638
13. LaCroix KJ, Tsui BM, Frey EC, Jaszczak RJ. Receiver operating characteristic evaluation of iterative reconstruction with attenuation correction in $^{99m}$Tc-sestamibi myocardial SPECT images. J Nucl Med 2000;41:502–513
14. Lalush DS, Frey EC, Tsui BM. Fast maximum entropy approximation in SPECT using the RBI-MAP algorithm. IEEE Trans Med Imaging 2000;19:286–294
15. Lalush DS, Tsui BM. Performance of ordered-subset reconstruction algorithms under conditions of extreme attenuation and truncation in myocardial SPECT. J Nucl Med 2000;41:737–744
16. Blankenberg F, Backer M, Patel V, Jehning B, Levashova Z, Backer J. Imaging of tumor angiogenesis with $^{99m}$Tc-labeled single chain (sc)VEGF. 2005: Late-Breaking Abstract Number: 585; 4th Annual Meeting of the Society of Molecular Imaging
17. Man S, Bocci G, Francia G, Green SK, Jothy S, Hanahan D, et al. Antitumor effects in mice of low-dose (metronomic) cyclophosphamide administered continuously through the drinking water. Cancer Res 2002;62:2731–2735
18. Emmenegger U, Man S, Shaked Y, Francia G, Wong JW, Hicklin DJ, et al. A comparative analysis of low-dose metronomic cyclophosphamide reveals absent or low-grade toxicity on tissues highly sensitive to the toxic effects of maximum tolerated dose regimens. Cancer Res 2004;64:3994–4000